Supporting Information

Synergistic OH^-/H^+ Modulation over Amorphous Gd_2O_3-Pt Interfaces for Efficient Alkaline Hydrogen Oxidation Reaction Electrocatalysis

Jingwen Zhang,[a] Mengjiao Liu,[a] Wenkang Lu,[a] Linbo Sun,[a] Yi Yang,[a] Jiawei Ke,[a] Jinjin Ding,*[a] Chenglin Yan,[b,c] Tongfei Li*[a] and Tao Qian[a]

[a]School of Chemistry and Chemical Engineering, Nantong University, Nantong 226019, China

[b]School of Petrochemical Engineering, Changzhou University, Changzhou 213164, China

[c]College of Energy, Key Laboratory of Core Technology of High Specific Energy Battery and Key Materials for Petroleum and Chemical Industry, Soochow University, Suzhou 215006, China

* E-mail: djjing@ntu.edu.cn (J. Ding); litongfei@ntu.edu.cn (T. Li)

Experimental section

Chemicals

Potassium tetrachloroplatinate (K_2PtCl_4), Gadolinium chloride ($GdCl_3$) and acetone were purchased from Sinopharm Chemical Reagent Co., Ltd. Ethanol (C_2H_5OH, 99.5 %), isopropanol (IPA, C_3H_8O, ACS, ≥99.5%) was obtained from Macklin. Carbon black (XC-72R) was attained from Carbot. Pt/C (20 wt%) and Nafion (5 wt%) were obtained from Sigma-Aldrich. All chemicals were employed without further purification.

Preparation of amorphous Gd_2O_3/C

200 mg of XC-72R and 300 mg of $GdCl_3$ were ultrasonicated in 30 mL of ethanol for 15 min, followed by the addition of 5 mL of water. The resulting mixture was heated to 80 °C under vigorous stirring for 8 h. Subsequently, the mixture was centrifuged and dried. The resultant material was calcined in a muffle furnace at 300 °C for 2 h to form amorphous Gd_2O_3/C. Finally, the product was washed with water and acetone, and then dried for further use.

Preparation of Pt-Gd_2O_3/C

24 mg of K_2PtCl_4 and 100 mg of the synthesized amorphous Gd_2O_3/C were dispersed in 50 mL of deionized water and ultrasonicated for 1 h. The resulting suspension was subsequently evaporated under reduced pressure using a rotary evaporator at 60 °C. The residue was collected and dried overnight at ambient conditions. Finally, the material was calcined in a H_2-Ar atmosphere at 300 °C for 1 h to obtain Pt-Gd_2O_3/C. The resultant product was washed sequentially with deionized

water and acetone, followed by drying under vacuum.

For comparison, Pt/C and Gd_2O_3/C catalysts were obtained using the identical procedure, except without the introduction of $GdCl_3$ and K_2PtCl_4, respectively, under the same conditions.

Material Characterization

The surface morphologies were characterized using scanning electron microscopy (SEM Sigma 500). The transmission electron microscopy (TEM) images were collected using a JEM-2100F TEM operating at 200 kV. High-angle annular dark-field scanning transmission electron microscopy (HAADF-STEM) images and energy-dispersive X-ray spectroscopy (EDS) mappings were obtained using the Titan Themis G2 STEM at 300 kV. The contact angle was measured using a contact drop angle measurement (JCY-1, FANGRUI). X-ray diffraction (XRD, Bruker D8 diffractometer) measurements were characterized with Cu Kα radiation (λ=1.54056 Å). Raman measurement of the nanocomposites was conducted on a Horiba (HR Evolution) using a 532 nm laser source. X-ray photoelectron spectroscopy (XPS) measurements were carried out at an Escalab Xi+X-ray photoelectron spectrometer using a monochromated aluminium Kα X-ray source at a pass energy of 187.85 eV, where the carbon 1s peak at 284.6 eV was taken as an internal standard. Ultraviolet photoelectron spectroscopy (UPS) spectra were recorded on a Thermo SCIENTIFIC ESCALAB Xi+analyzer with He I light source (hυ = 21.22 eV). The Pt content was determined by an inductively-coupled plasma mass-spectrometer (Agilent 8900x QQQ-ICP-MS, Agilent, USA).

Electrochemical measurements

Electrochemical measurements were performed on a CHI 660E workstation (Shanghai Chenhua Instrument Corporation, China) in a 0.1 M KOH solution using a three-electrode system. A graphite rod and an Hg/HgO electrode (saturated KCl) were used as the counter and reference electrodes, respectively. The rotating disk electrode (RDE) assembly (AFE7R9GCPT, Pine Research Instrumentation, USA) consisted of a rotation disk electrode. To prepare the catalyst ink, 5 mg of catalyst was mixed with 100 μL Nafion solution (5 wt. %), followed by the addition of 300 μL deionized water and 600 μL ethanol. After 30 min sonication, 10 μL catalyst ink was deposited onto a glassy carbon electrode (diameter 5 mm, geometric area: 0.196 cm^2), which was used as a working electrode after dried at room temperature. Cyclic voltammetry (CV) curves were recorded on the RDE in H_2-saturated 0.1 M KOH electrolyte at a scan rate of 50 mV/s from 0.02 to 1.02 V (vs. RHE). Linear sweep voltammetry (LSV) curves were obtained on the RDE in H_2-saturated electrolyte with a scan rate of 1 mV s^{-1} from -0.05 to 0.25 V (vs. RHE) at a rotation speed of 1600 rpm. Electrochemical impedance spectroscopy (EIS) was performed from 100 kHZ to 0.01 HZ at open circuit voltage with an amplitude of 5 mV. CO stripping voltammetry was conducted in 0.1 M KOH solution with the CV measurement. Prior to the test, the electrolyte was purged with pure N_2 to get rid of dissolved air in the electrolyte. Subsequently, the electrode was kept at 0.1 V vs. RHE for 15 min while bubbling CO gas. Following this, the electrolyte was purged with N_2 for 30 min to ensure complete remove of CO. CO stripping voltammetry was recorded from 0 V to 1.2 V (vs. RHE) at 20 mV s^{-1}. All potentials were calibrated relative to the reversible hydrogen electrode (RHE) scale according to the Nernst equation ($E_{RHE} = E_{Hg/HgO} + 0.059 \times pH + 0.1989$ V), where $E_{Hg/HgO}$ is the external potential measured against the Hg/HgO reference electrode.

AEMFC tests

5 mg of Pt-Gd_2O_3/C was added into mixture solution containing of IPA, DI water, and Nafion to prepare the catalyst ink. Subsequently, the as-made ink was brush painted on one side of anion exchange membrane (Fuma 3-50) to form the anode catalyst layer. Commercial 40 wt% Pt/C (Johnson Matthey) was used as a cathode catalyst for forming the cathode catalyst layer on the opposite side of the membrane. The catalyst-coated membranes (CCMs) with an active area of 4 cm^2 were then sandwiched between two gas diffusion layers (GDLs). The fuel cell performance was examined at 40 ^{o}C under humidified H_2 and O_2 flow rates of 100 sccm at 80% relative humidity, with a back pressure of 150 kPa.

Figures and Tables

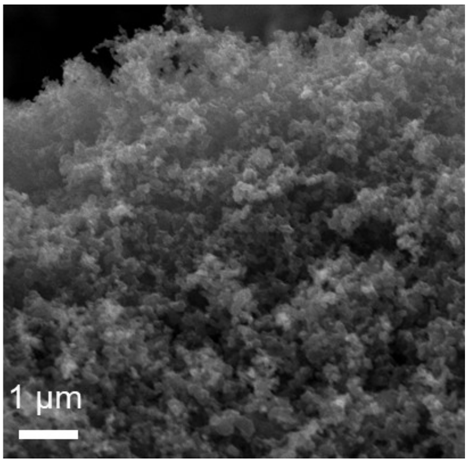

Fig. S1 SEM image of Pt-Gd_2O_3/C.

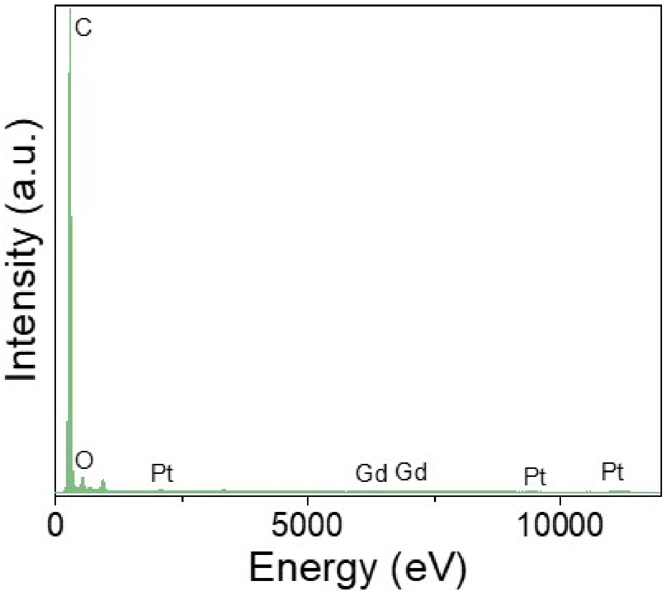

Fig. S2 EDS spectrum of Pt-Gd_2O_3/C.

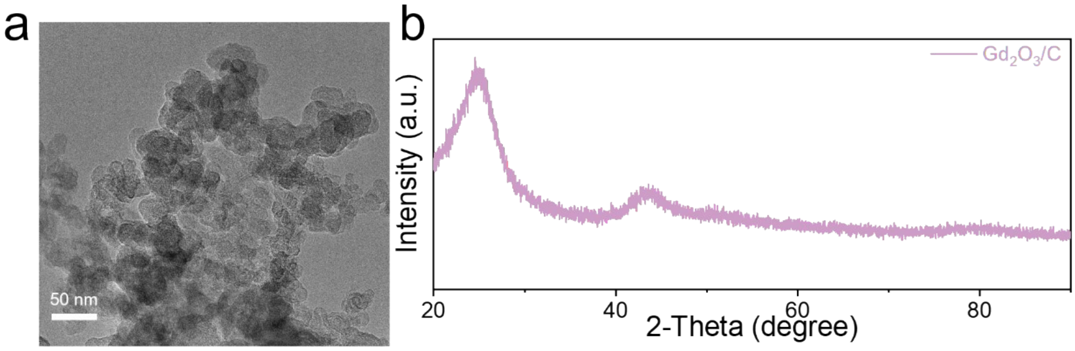

Fig. S3 (a) TEM image, and (b) XRD pattern of Gd_2O_3/C.

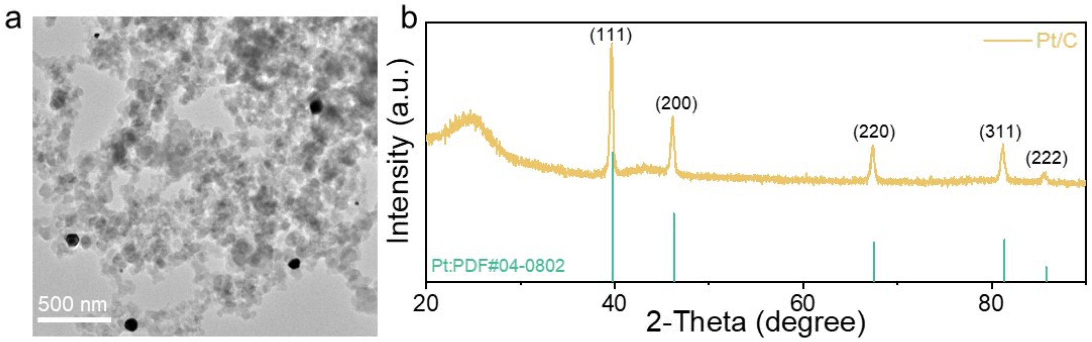

Fig. S4 (a) TEM image of Pt/C. (b) XRD pattern of Pt/C.

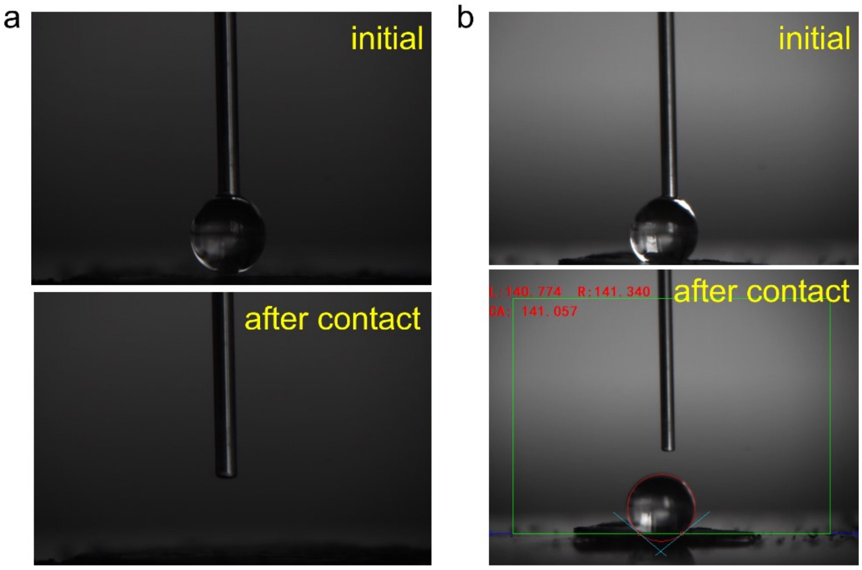

Fig. S5 (a) Contact angle measurement of Pt/C. (b) Contact angle measurement of Gd_2O_3/C.

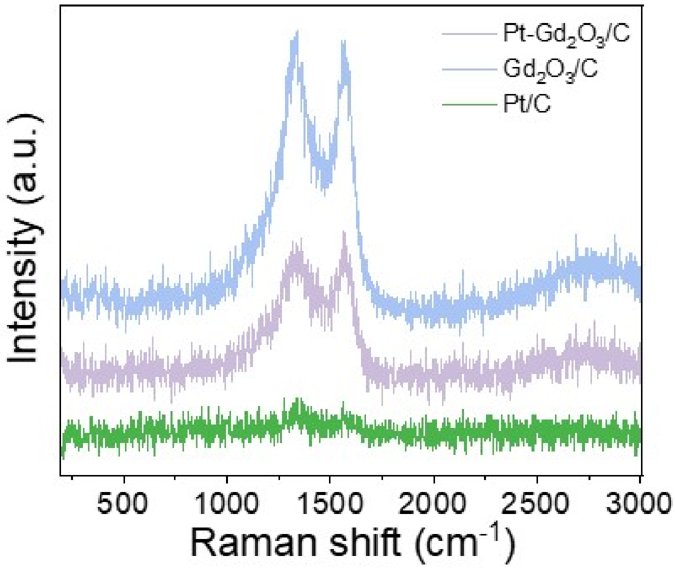

Fig. S6 The Raman spectra of Pt-Gd$_2$O$_3$/C, Gd$_2$O$_3$/C and Pt/C.

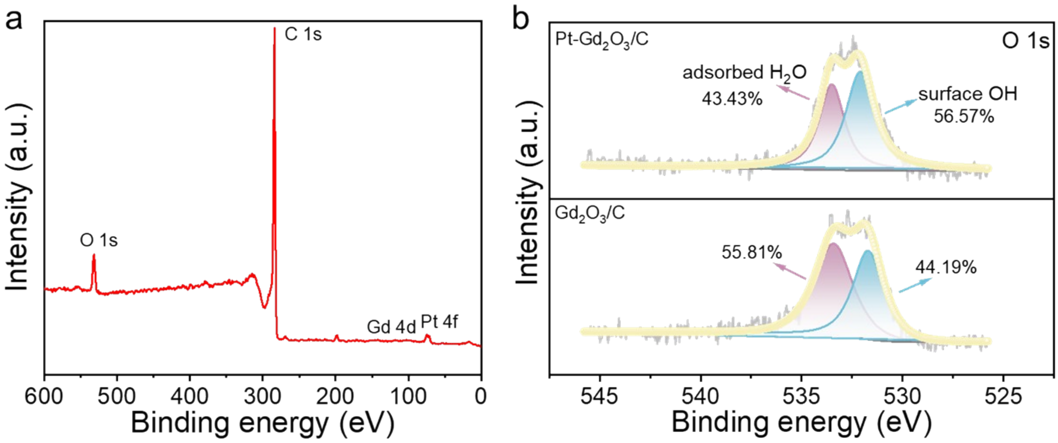

Fig. S7 The XPS survey spectrum of Pt-Gd_2O_3/C.

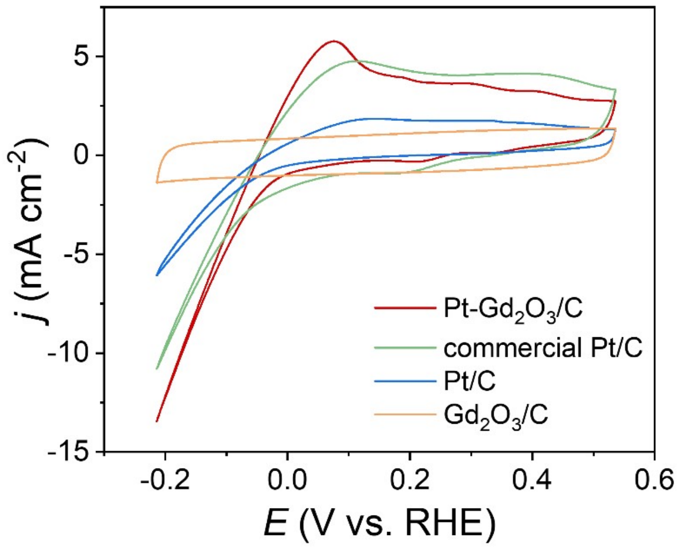

Fig. S8 CV curves of Pt-Gd$_2$O$_3$/C, commercial Pt/C, Pt/C and Gd$_2$O$_3$/C catalysts in H$_2$ atmosphere.

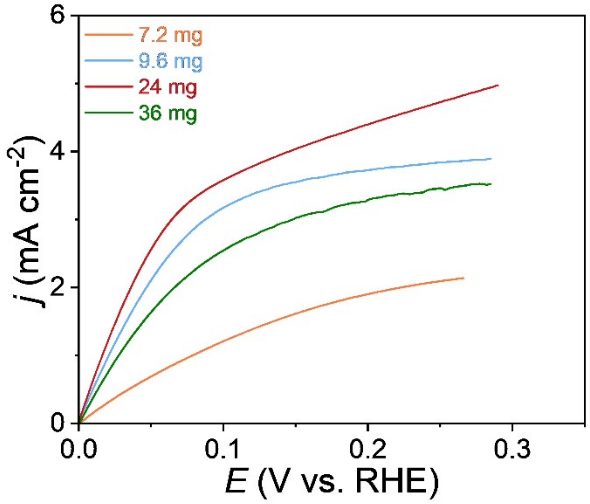

Fig. S9 LSV curves of different Pt-loading Pt-Gd_2O_3/C.

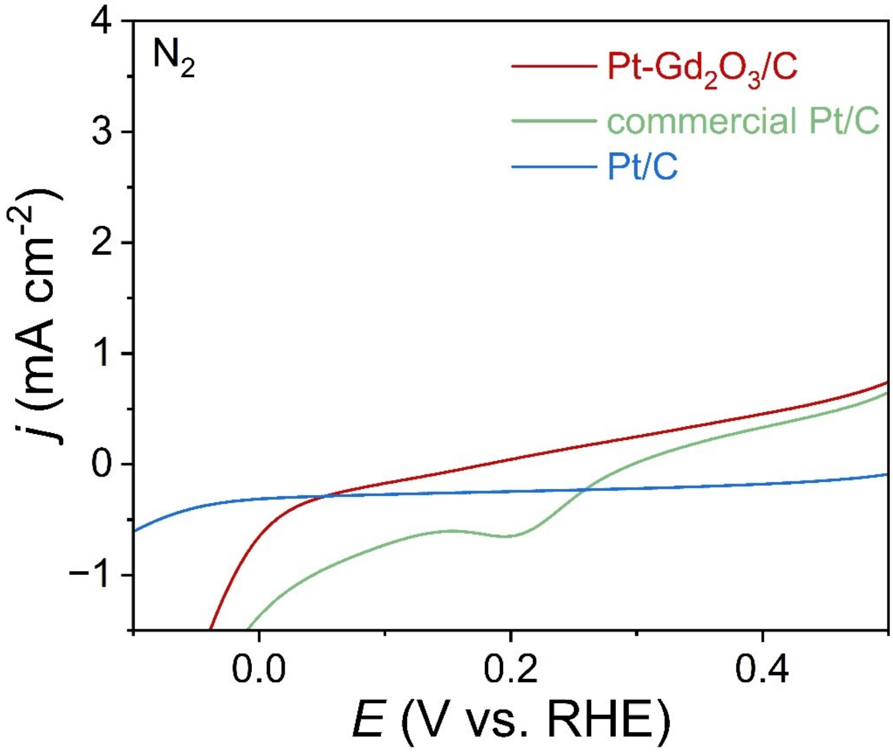

Fig. S10 LSV curves of different samples in N_2-saturated 0.1 M KOH solution.

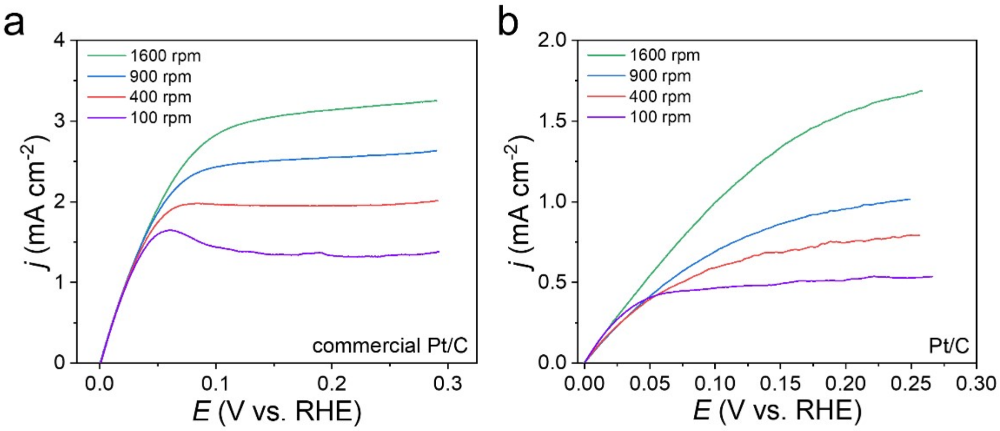

Fig. S11 (a) Polarization curves of commercial Pt/C at different rotation rates. (b) Polarization curves of Pt/C at different rotation rates.

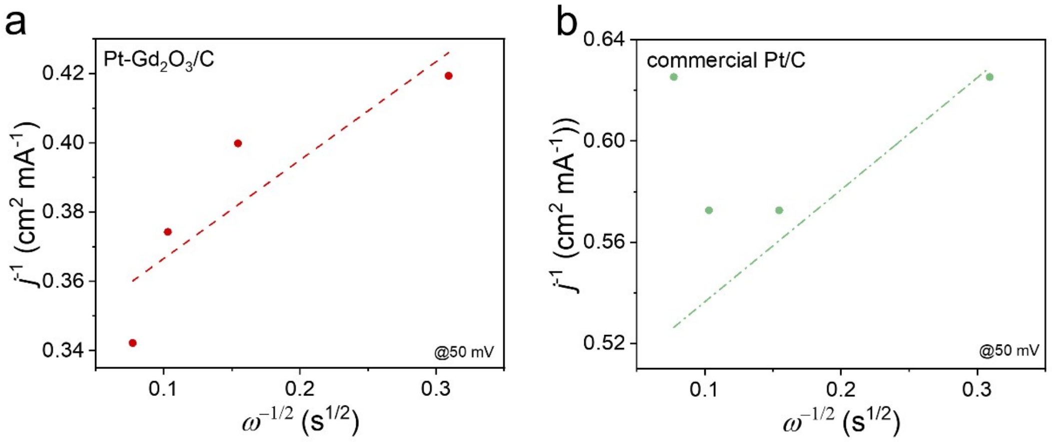

Fig. S12 (a) The Koutecky–Levich plot of Pt-Gd_2O_3/C at an overpotential of 50 mV. (b) The Koutecky–Levich plot of commercial Pt/C at an overpotential of 50 mV.

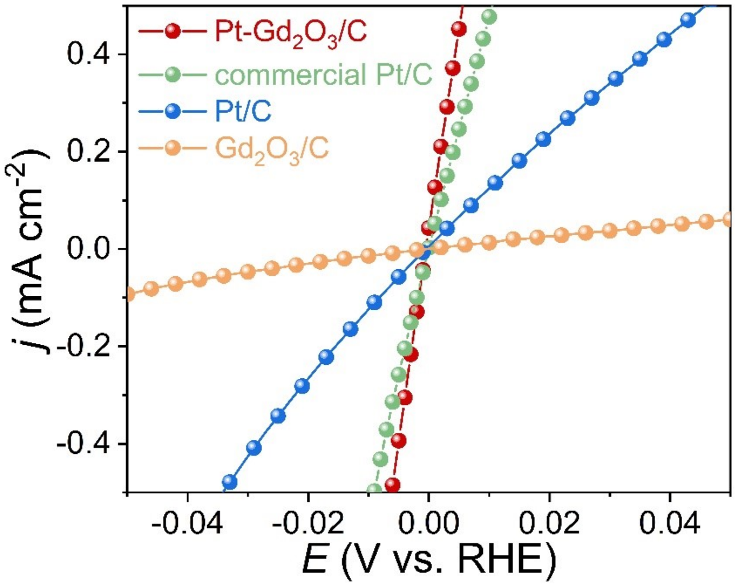

Fig. S13 Linear current potential region around the equilibrium potential.

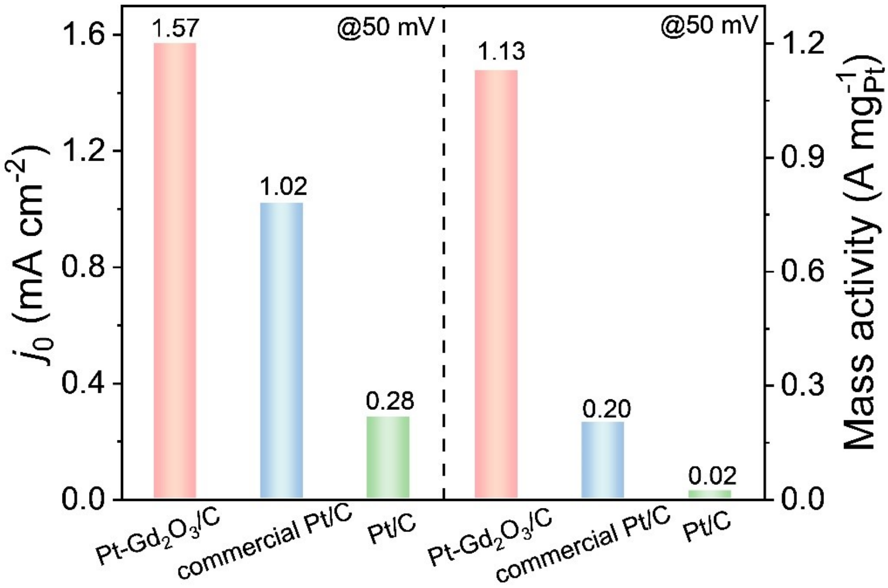

Fig. S14 Comparison of j_0 and mass activity at an overpotential of 50 mV.

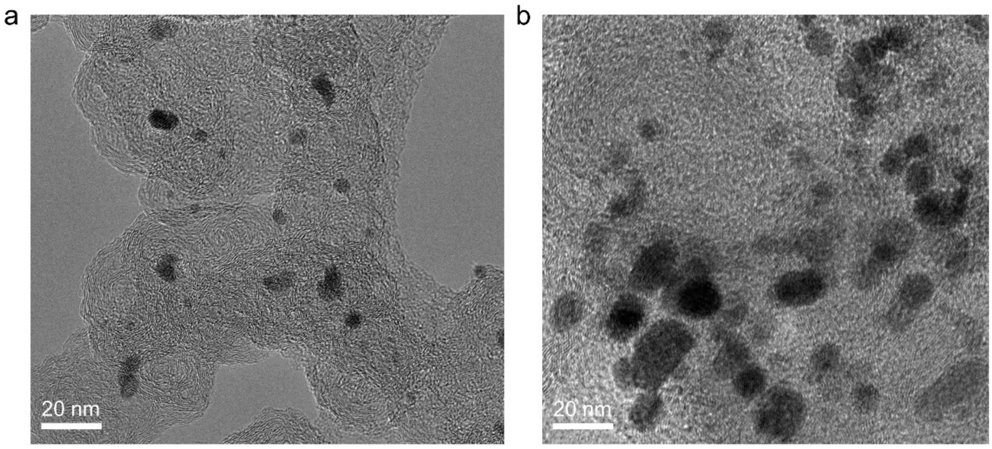

Fig. S15 (a)TEM image of Pt-Gd_2O_3/C after HOR stability measurement. (b)TEM image of Pt-Gd_2O_3/C after stability test of AEMFCs.

Table S1. Pt and Gd content (wt%) of samples determined using ICP-OES.

Element	Pt-Gd_2O_3/C	Pt /C
Pt (ωt. %)	13.60	1.85
Gd (ωt. %)	4.74	-

Table S2. Comparison of the HOR activity of Pt-Gd_2O_3/C with other advanced electrocatalysts reported previously.

Number	Catalyst	j_k (mA cm^{-2})@50mV	Ref
1	Pt-Gd_2O_3/C	39.36	This work
2	Commercial Pt/C	6.94	This work
3	Pt/C	0.68	This work
4	Pt/Cu NWs	10.9	1
5	Ru@N-CNFs	2.73	2
6	Eu_2O_3@N-CNFs	3.27	2
7	Ni/N-CNT	2.33	3
8	Ni_3N/C	3.9	4
9	Ni/CeO_2/C	1.73	5
10	Ni/NiO/C	1.59	6
11	$MoNi_4$	33.8	7
12	WNi_4	8.31	7
13	np-Ni_3N	4.76	8
14	Ir/C-800C	4.1	9
15	PtRuTe	4.05	10

Table S3. Comparison with other recently reported Pt-based catalysts in terms of chronoamperometry in 0.1 M KOH electrolyte at pure H_2-saturated atmosphere.

Number	Catalyst	Relative current (%)	Time	Ref
1	Pt-Gd_2O_3/C	87.47	80000s	This work
2	Pt/C	67.32	50000s	This work
3	GCN-Tb-Pt	67.5	3h	[11]
4	Pt-GCN	63.3	3h	[11]
5	PtIrFeCoNiMo	84.23	20000s	[12]

Table S4. Comparison with other recently reported Pt-based catalysts in terms of MA in 0.1 M KOH electrolyte.

Number	Catalyst	Overpotential (mV)	MA (mA mg^{-1}_{Pt})	Ref
1	Pt-Gd_2O_3/C	50	1130	This work
2	Pt/C	50	200	This work
3	LD-Pt WNPs	50	968.5	[13]
4	$Pt_{0.9}$ $Pd_{0.1}$ /C	50	255	[14]
5	$(Pt_{0.9}Pd_{0.1})_3Fe$/C	50	326.1	[14]
6	PtCu NWs	50	660	[15]
7	PtRu/Mo_2C-TaC	25	403	[16]
8	PtRu NWs	50	600	[17]
9	Pd_3Co@Pt/C	25	685	[18]
10	Pd_3Fe@Pt/C	25	661	[18]
11	Pt/NiO	50	200	[19]
12	Pt-(PtOx)-NSs/C	50	500	[20]
13	Ru@Pt NPs	50	1030	[21]

References

[1] S. Alia, B. Pivovar and Y. Yan, *J. Am. Chem. Soc.*, 2013, **135**, 13473-13478.

[2] L. Zhang, S. Chen, T. Du, X. Zhao, A. Dong, L. Zhang, T. Li, C. Yan, and T. Qian, *ACS Nano*, 2024, **18**, 34195–34206.

[3] Z. Zhuang, S. Giles, J. Zheng, G. Jenness, S. Caratzoulas, D. Vlachos and Y. Yan, *Nat. Commun.*, 2016, **7**, 10141.

[4] W. Ni, A. Krammer, C. Hsu, H. Chen, A. Schuler and X. Hu, *Angew. Chem. Int. Ed.*, 2019, **58**, 7445-7449.

[5] F. Yang, X. Bao, P. Li, X. Wang, G. Cheng, S. Chen and W. Luo, *Angew. Chem. Int. Ed*. 2019, **58**, 14179-14183.

[6] Y. Yang, X. Sun, G. Han, X. Liu, X. Zhang, Y. Sun, M. Zhang, Z. Cao and Y. Sun, *Angew. Chem. Int. Ed.,* 2019, **58**, 10644-10649.

[7] Y. Duan, Z. Yu, L. Yang, L. Zheng, C. Zhang, X. Yang, F. Gao, X. Zhang, X. Yu, R. Liu, H. Ding, C. Gu, X. Zheng, L. Shi, J. Jiang, J. Zhu, M. Gao and S. Yu, *Nat. Commun.*, 2020, **11**, 4789.

[8] T. Wang, M. Wang, H. Yang, M. Xu, C. Zuo, K. Feng, M. Xie, J. Deng, J. Zhong, W. Zhou, T. Cheng and Y. Li, *Energy Environ. Sci.*, 2019, **12**, 3522-3529.

[9] J. Zheng, Z. Zhuang, B. Xu and Y. Yan, *ACS Catal.*, 2015, **5**, 4449-4455.

[10] S. Ma, T. Ma, Q. Hu, H. Yang and C. He, *Sci. China Mater.*, 2022, **65**, 3462-3469.

[11] Y. Chen, M. Yuan, Y. Yang, X. Liu, L. Lin, Z. Liang, R. Gao, Z. Tao, P. Wang, H. Guo, Y. Liu and X. Zheng, *Nano Research*, 2025, **18**, 94907349.

[12] X. Ma, S. Zhang, Y. Zhou, W. Lei, Y. Zhai, Y. Zhao and C. Shan, *J. Mater. Chem. A*,2024, **12**,8862–8868.

[13] X. Li, X. Han, Z. Yang, S. Wang, Y. Yang, J. Wang, J. Chen, Z. Chen and H. Jin, *Nano Res.*, 2024, **17**, 3819–3826.

[14] T. Zhao, G. Wang, M. Gong, D. Xiao, Y. Chen, T. Shen, Y. Lu, J. Zhang, H. Xin, Q. Li and D. Wang, *ACS Catal.,* 2020, **10**, 15207.

[15] S. M. Alia, B. S. Pivovar and Y. Yan, *J. Am. Chem. Soc.*, 2013, **135**, 13473.

[16] E. Hamo, R. Singh, J. Douglin, S. Chen, M. Hassine, E. Carbo-Argibay, S. Lu, H.

Wang, P. Ferreira, B. Rosen and D. Dekel, *ACS Catal.,* 2021, **11**, 932.

[17] M. Scofield, Y. Zhou, S. Yue, L. Wang, D. Su, X. Tong, M. B. Vukmirovic, R. R. Adzic and S. S. Wong, *ACS Catal.*, 2016, **6**, 3895.

[18] T. Zhao, Y. Hu, M. Gong, R. Lin, S. Deng, Y. Lu, X. Liu, Y. Chen, T. Shen, Y. Hu, L. Han, H. Xin, S. Chen and D. Wang, *Nano Energy*, 2020, **74**, 104877.

[19] G. Zhao, L. Xia, P. Cui, Y. Qian, Y. Jiang, Y. Zhao, H. Pan, S. X. Dou and W. Sun, *Nano Lett.,* 2021, **21**, 4845.

[20] M. Kundu, T. Bhowmik, R. Mishra and S. Barman, *ChemSusChem*, 2018, **11**, 2388–42401.

[21] K. Elbert, J. Hu, Z. Ma, Y. Zhang, G. Chen, W. An, P. Liu, H. Isaacs, R. Adzic and J. Wang, *ACS Catal.*, 2015, **5**, 6764.